Proc. Natl. Acad. Sci. USA
Vol. 94, pp. 3903–3908, April 1997
Immunology

Subtractive isolation of phage-displayed single-chain antibodies to thymic stromal cells by using intact thymic fragments

(thymus/T cell differentiation/immunohistology/epithelium)

WILLEM VAN EWIJK*†, JOHN DE KRUIF‡, WILFRED T. V. GERMERAAD*, PAUL BERENDES*, CARSTEN RÖPKE§, PETER PAUL PLATENBURG*, AND TON LOGTENBERG‡

*Department of Immunology, Erasmus University of Rotterdam, Dr. Molewaterplein 50, 3015 GE Rotterdam, The Netherlands; ‡Department of Immunology, University Hospital Utrecht, Medical School, Heidelberglaan 100, 3584 CX Utrecht, The Netherlands; and §Laboratory of Cellular Immunology, Department of Medical Anatomy, University of Copenhagen, The Panum Institute, Blegdamsvej 3, DK-2200 Copenhagen N, Denmark

Communicated by Hugh O. McDevitt, Stanford University School of Medicine, Stanford, CA, November 26, 1996 (received for review September 26, 1996)

ABSTRACT **In the murine thymus, the stroma forms microenvironments that control different steps in T cell development. To study the architecture of such microenvironments and more particularly the nature of communicative signals in lympho–stromal interaction during T cell development, we have employed the phage antibody display technology, with the specific aim of isolating thymic stromal cell-specific single-chain antibodies from a semisynthetic phage library. A subtractive approach using intact, mildly fixed thymic fragments as target tissue and lymphocytes as absorber cells generated monoclonal phages (MoPhabs) detecting subsets of murine thymic stromal cells. In the present paper we report on the reactivity of single-chain antibodies derived from three MoPhabs, TB4–4, TB4–20, and TB4–28. While TB4–4 and TB4–20 are both epithelium specific, TB4–28 detects an epitope expressed on both epithelial- and mesenchymal-derived stromal cells. TB4–4 reacts with all cortical epithelial cells and with other endoderm-derived epithelia, but this reagent leaves the majority of medullary epithelial cells unstained. In contrast, MoPhab TB4–20 detects both cortical and medullary thymic epithelial cells, as well as other endoderm- and ectoderm-derived epithelial cells. Cross-reaction of single-chain antibodies to human thymic stromal cells shows that our semisynthetic phage antibody display library, in combination with the present subtractive approach, permits detection of evolutionary conserved epitopes expressed on subsets of thymic stromal cells.**

The differentiation of T lymphocytes in the thymus depends on intimate cellular communication between developing thymocytes and stromal cells (1). While migrating through the thymus, developing T cells sequentially interact with various types of mesenchymal, epithelial, and bone-marrow-derived cells that collectively constitute the unique three-dimensionally oriented microenvironments in the thymic stroma (2). Such lympho–stromal interactions result in proliferation, differentiation, and selection of thymocytes, generating a repertoire of mature T cells equipped with appropriate T cell receptors (3, 4).

We have recently provided evidence that lympho–stromal interaction in the thymus is reciprocal in nature: stromal cells influence T cell differentiation, but in turn, developing T cells influence the composition and differentiation of thymic microenvironments (5, 6). This latter phenomenon, for which the term "thymic crosstalk" has been coined (7), occurs at various stages in T cell development, and it can be visualized in mice in which T cell differentiation has been blocked by genetic manipulation. Collectively, these data indicate that the unique three-dimensional architecture of the thymic microenvironments plays a central role in lympho–stromal interaction during T cell development.

To study the differentiation, composition, and functional role of thymic microenvironments in T cell development, monoclonal antibodies specific for subsets of thymic stromal cells have been generated (reviewed in ref. 8). However, with the exception of monoclonal antibodies directed to major histocompatibility complex (MHC) antigens (9), and the T cell receptor–CD3 complex (10, 11), none of the currently available anti-stromal antibodies influence the development of thymocytes or stromal cells, when tested *in vitro* or *in vivo* models, precluding further analysis of the molecules involved in lympho–stromal interaction. To search for molecules expressed in the native configuration of the thymic stroma, we have applied a recently developed subtractive approach that permits the selection of single-chain Fv antibodies (scFv) with desirable binding specificities from libraries of antibodies displayed on the surface of filamentous phage particles (12, 13). Intact, mildly fixed murine thymic tissue fragments, from which T cells had been largely removed, were used as targets for a large synthetic phage display library. This library was preadsorbed with thymocytes and spleen cells to remove undesired specificities. After four rounds of selection, monoclonal antibody phages (MoPhabs) were obtained that, when tested in immunohistology, displayed binding to subsets of thymic stromal cells. This protocol sets the stage for the isolation of novel antibody specificities directed against molecules relevant in thymic "crosstalk."

MATERIALS AND METHODS

Mice. Male and female C57BL6 ($H2^b$), BALB/c ($H2^d$), C3H ($H2^k$), and (C57BL × CBA) F_1 ($H2^{bk}$) mice were kept at routine specific-pathogen-free conditions in our animal colonies.

Stromal Cells and Stromal Cell Cultures. Stromal cells were isolated from thymic lobes derived from 14-day-old C3H embryos, essentially as described before (14).

Phage Antibody Library. The semisynthetic phage antibody display library of human scFv antibody fragments has been described in detail elsewhere (12, 13).

Antibodies and Conjugates. Antibodies used in the present study were as follows: sheep-anti phage M13 polyclonal antibodies, conjugated to horseradish peroxidase (HRP) (Pharmacia), mouse monoclonal antibodies directed to the Myc tag expressed by scFvs, (9E10; American Type Culture Collection), rat monoclonal antibodies directed to subsets of thymic stromal cells

The publication costs of this article were defrayed in part by page charge payment. This article must therefore be hereby marked "*advertisement*" in accordance with 18 U.S.C. §1734 solely to indicate this fact.

0027-8424/97/943903-6$2.00/0
PNAS is available online at **http://www.pnas.org**.

Abbreviations: MHC, major histocompatibility complex; scFv, single-chain Fv antibody; MoPhab, monoclonal phages expressing an scFv; HRP, horseradish peroxidase; FITC, fluorescein isothiocyanate; CLSM, confocal laser scanning microscopy.

†To whom reprint requests should be addressed.

(ERTR4, ERTR5, and ERTR7; ref. 15), rabbit anti-mouse Ig HRP conjugate (Dako), rabbit anti-rat Ig HRP conjugate (Dako), rabbit anti-rat Ig labeled with fluorescein isothiocyanate (FITC) (Dako), rabbit anti-mouse Ig labeled with FITC (Dako), and goat anti-mouse conjugate with alkaline phosphatase (Tago). FITC-labeled streptavidin (Zymed) was also used.

Preparation of Tissues for Phage Selection. To prepare stromal cells for phage selection, we mildly fixed thymic tissue with a solution of 0.05% glutaraldehyde (Polysciences) in PBS, using total body perfusion fixation (16). After 10 min of perfusion, the thymus was isolated and minced with scissors. Nonadherent thymocytes were removed by vigorously shaking the thymic fragments in PBS, using a Vortex mixer. Thymic fragments were stored at 4°C in PBS containing 1% fetal calf serum (PBS-FCS). Fixed thymocytes were centrifuged and brought into suspension in PBS-FCS. For absorption purposes, spleen cells were collected, fixed, and stored as described above.

Isolation of a Thymic Stroma-Specific Phage Library. A 400-μl portion of the stock phage library (approximately 10^{13} phages per ml) was added to 1 ml of PBS containing 4% low-fat milk powder (M-PBS). To this solution, 1 ml of M-PBS, containing 2.5×10^8 0.05% glutaraldehyde-fixed adsorber cells (thymocytes + spleen cells), was added and allowed to incubate for 1 hr at room temperature. At the same time, fixed thymic fragments were preincubated with 1 ml of M-PBS in a 5-ml polystyrene tube. After 1 hr, adsorber cells were removed by centrifugation and the adsorbed phage library was transferred to the 5-ml tube containing the thymic fragments. To this mixture, 2.5×10^8 freshly fixed adsorber cells were added. The mixture was incubated overnight at 4°C, with slow rotation. The following day thymic fragments were allowed to sediment, the supernatant was decanted, and the thymic fragments were vigorously rinsed, using a total volume of 2 liters of M-PBS containing 0.05% Tween 20 (M-PBS-Tw), to remove nonspecifically adhered phages. To elute specifically bound phages, thymic fragments were transferred in a volume of 300 μl of M-PBS-Tw to a 15-ml tube containing 450 μl of sodium citrate (pH 2.5). After 5 min, the pH was neutralized by adding 375 μl of 1 M Tris·HCl buffer (pH 7.4). Finally, 3 ml of 2TY medium (GIBCO/BRL) and 3 ml of *Escherichia coli* XL-1 blue (Stratagene) was added. Infection was allowed to proceed for 30 min. Bacteria were centrifuged at $2,200 \times g$ for 30 min, suspended in 0.5 ml of 2TY, and plated on agar plates containing 25 μg/ml tetracycline, 100 μg/ml ampicillin, and 5% glucose (TAG). After overnight culture at 37°C, plates were scraped and bacteria were frozen in stock vials or used to prepare the next library as described in detail elsewhere (13). In each selection round, thymic fragments from a different mouse strain were used.

Isolation of Stroma-Specific MoPhabs. After four rounds of subtractive selections, individual bacterial colonies were picked and cultured in a final volume of 50 ml of 2TY-TAG. Helper phages were added to each culture and phages were harvested from the supernatant by two subsequent precipitation rounds using polyethylene glycol/NaCl, as described (13).

Electron Microscopy. M13 bacteriophages were allowed to adhere to Formvar-coated grids, fixed in 1% glutaraldehyde in PBS for 5 min at room temperature, washed in PBS for 5 min, and incubated with sheep anti-M13 HRP conjugate, followed by incubation with diaminobenzidene.

Immunohistochemistry with MoPhabs. Binding of MoPhabs to thymic stroma was determined by immunohistological screening. Frozen sections 5 μm thick were incubated with MoPhab solutions in a moist chamber for 30 min. Nonadherent phages were removed by vigorously rinsing the slides in M-PBS-Tw. Bound MoPhabs were visualized by incubation of the sections with a 1:50-diluted sheep anti-M13 HRP conjugate, followed by incubation with diaminobenzidene. MoPhabs showing reticular staining patterns were recloned and frozen in stocks at −70°C.

Production and Purification of scFvs and Bivalent Antibodies. Single-chain fragments were produced in the *E. coli* nonsuppressor strain SF110, as described (13). The SF110 strain is deficient in the DegP and OmpT proteases resulting in the production of stable scFv fragments. In addition, plasmids of MoPhab TB4–4, TB4–20, and TB4–28 were digested with *Not*I and *Nco*I, and the coding regions for the scFv were subcloned in the *Not*I/*Nco*I-digested vector 1M3-HIS that adds 6 histidine residues (His-tag) to the carboxyl terminus of the scFv fragment. These constructs were introduced into *E. coli* SF110 and His-tagged scFvs were produced (17). Periplasmic preparations of scFvs were purified over a Ni–NTA-agarose column (Qiagen) and eluted by imidazole competition into 2-ml fractions. Purity of the scFvs was confirmed by standard SDS/PAGE electrophoresis, followed by Coomassie brilliant blue staining.

Immunohistochemistry with scFvs. To determine the reactivity of scFvs, 5-μm frozen sections of various organs (see also Table 1) were incubated with purified scFvs for 30 min at room temperature. Next, sections were rinsed thoroughly in M-PBS/Tw under continuous stirring. As a second step, a mouse anti-Myc monoclonal antibody (clone 9E10) was added, and sections were incubated for another 30 min. After extensive rinsing with M-PBS/Tw, sections were incubated with 1:300-diluted rabbit anti-mouse-Ig-peroxidase. This conjugate was stained by using diaminobenzidene.

Confocal Laser Scanning Microscopy (CLSM). To study thymic tissue in CLSM, 25-μm frozen sections were cut and briefly dipped in acetone. Sections were incubated with scFvs, followed by supernatant from 9E10 and a 1:100-diluted FITC-labeled rabbit anti-mouse Ig antiserum. Digital fluorescence images were recorded with a Zeiss CLSM 410 Invert confocal microscope, equipped with an air-cooled 488-nm argon laser.

Immunoblotting with scFvs and $(scFv)_2$ Antibodies. To determine the molecular weight of the proteins detected by scFvs, immunoblotting was performed on thymic stromal cells collected by mincing the thymus through a nylon sieve. The sieve was cut into fragments and incubated in SDS sample buffer. Samples were prepared for immunoblotting as described before (18).

Fingerprinting and Nucleotide Sequence Analysis. The diversity of phages displaying binding activity to thymic stromal cells was assessed by *Bst*NI DNA fingerprint analysis of

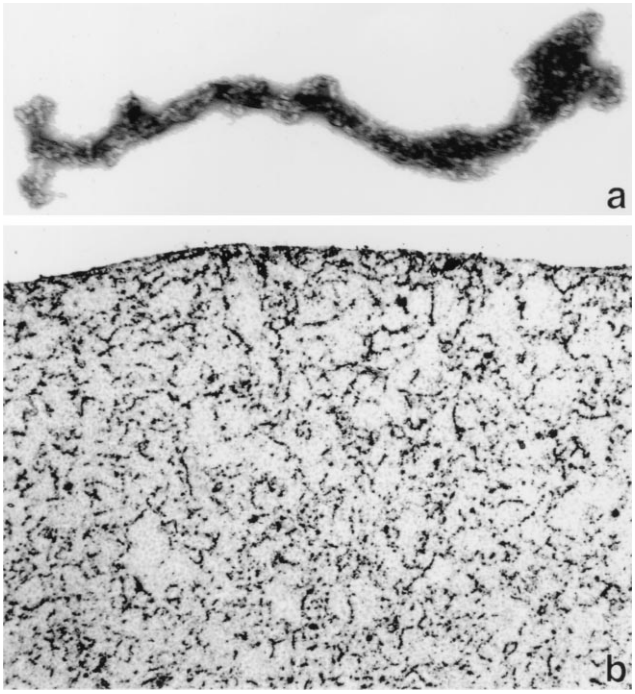

FIG. 1. (*a*) Transmission electron micrograph of a TB4–4 MoPhab. (×39,000.) (*b*) Light micrograph of a frozen section of the BALB/c thymus incubated with TB4–4 MoPhab. (×120.)

individual phage MoPhabs as described (19). The nucleotide sequence of individual MoPhabs was determined with the Applied Biosystems Prism Dye Terminator Cycle Sequencing Kit (Perkin–Elmer), using the primers LINKSEQ and PHENSEQ on an automated sequencer.

RESULTS

Experimental Strategy. To direct the selection of MoPhabs to stromal cells, we preadsorbed the library with thymocytes and spleen cells from the same mouse strains, before and during incubation with thymic fragments. To avoid isolation of phages directed to MHC antigens, we altered the MHC haplotype in each selection round. After four rounds, individual colonies were picked for production of MoPhabs.

Reactivity of MoPhabs in Immunohistology. MoPhabs were visualized by incubation with a sheep anti-M13–peroxidase conjugate, followed by incubation with diaminobenzidene. This procedure labels the entire phage particle (Fig. 1*a*). As an example for the immunohistological detection of specific phage binding, Fig. 1*b* shows the reactivity of the MoPhab TB4–4, as detected on a frozen section of the murine thymus. A specific reticular staining pattern can be observed, indicative for reactivity of this MoPhab with cortical epithelial cells. From a number of MoPhabs reacting in similar patterns, scFvs were prepared and tested in immunohistology (Figs. 2 and 3).

Immunohistology of scFvs with Lymphoid Tissue. Immunohistological analysis of mouse and human thymus sections incubated with scFvs, from MoPhabs TB4–4, TB4–20, and TB4–28 showed three different reticular staining patterns, as illustrated in Fig. 2. ScFvs obtained from MoPhab TB4–4 react with all cortical epithelial cells and with a minor subpopulation of medullary stromal cells in the murine thymus (Fig. 2*a*). These antibodies crossreact only to a minor extent with subsets of cortical epithelial cells in the human thymus (Fig. 2*b*). In contrast, scFvs from MoPhab TB4–20 react both with all cortical and with all medullary epithelial reticular cells in the murine thymus (Fig. 2*c*). These scFvs strongly crossreact to human thymic epithelial cells, present in both cortex and medulla; they also detect Hassal's corpuscles (Fig. 2*d*). ScFvs from MoPhab TB4–28 react with subsets of epithelial reticular cells in both the cortex and the medulla (Fig. 2*e*). These scFvs do not crossreact to human thymic tissue (Fig. 2*f*).

In our immunohistological analysis of peripheral lymphoid tissues, we observed that from the three scFvs only TB4–28 scFvs react with cell types in peripheral lymphoid organs. These antibodies exclusively detect endothelial cells of high

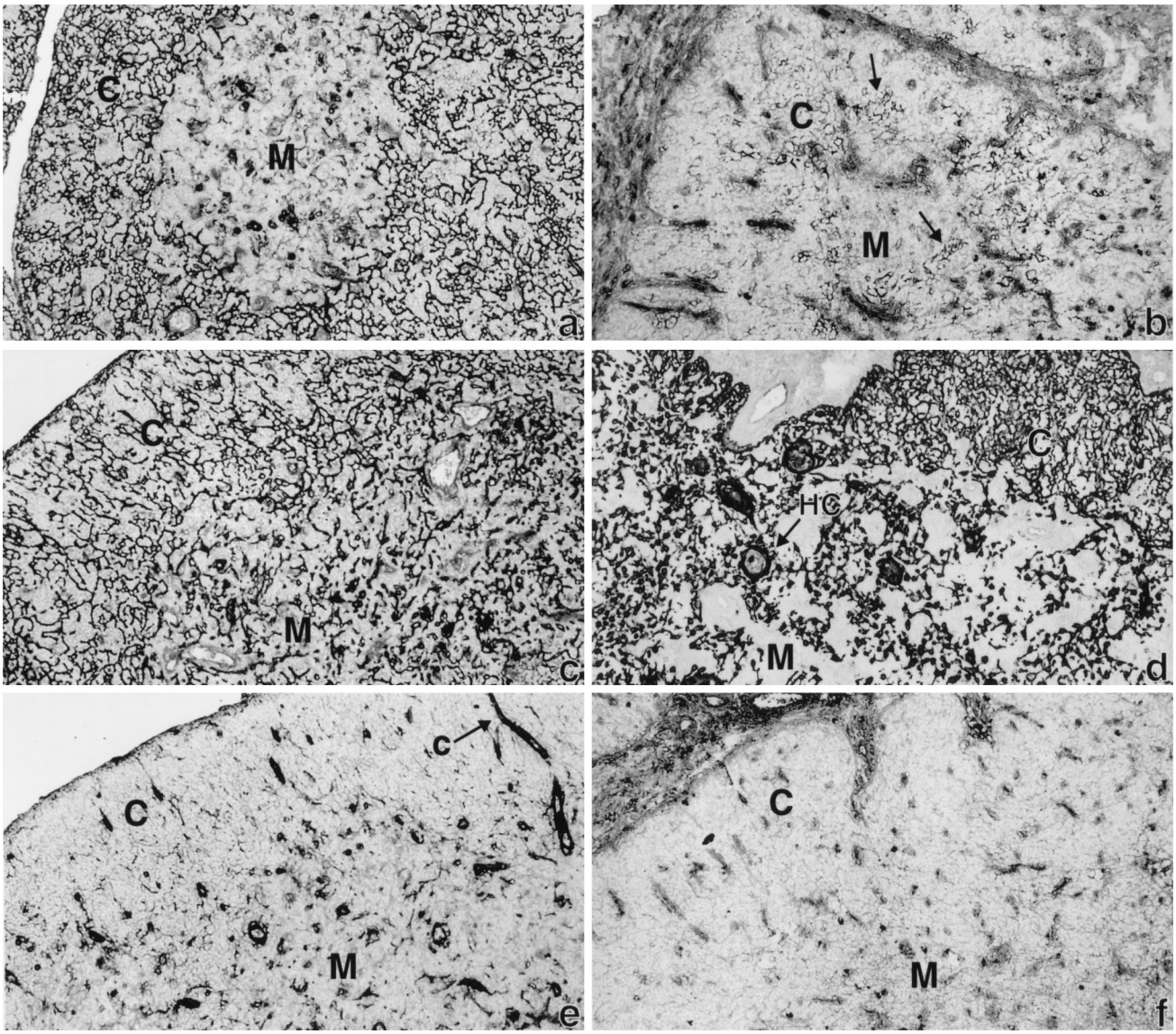

FIG. 2. Frozen sections of mouse thymus (*a*, *c*, and *e*) and human thymus (*b*, *d*, and *f*) incubated with scFvs derived from MoPhabs TB4–4 (*a* and *b*), TB4–20 (*c* and *d*), and TB4–28 (*e* and *f*). C, cortex; M, medulla; HC, Hassal's corpuscle; c, capillary. (×105.)

Table 1. Reactivity of single-chain antibodies

Organ	Reactivity with MoPhab		
	TB4-4	TB4-20	TB4-28
Lymphoid			
Thymus	+[a]	+[b]	+[c]
Lymph node	−	−	+[d]
Spleen	−	−	−
Nonlymphoid			
Skin	−	+[e]	+[f]
Duodenum	+[g]	+[h]	+[i]
Liver	+[j]	+[j]	+[j]
Pancreas	+[k]	+[k]	+[l]
Kidney	+[m]	+[m]	+[n]
Testis	−	−	+[o]
Lung	+[p]	+[q]	ND
Mandibular gland	+[i]	+[i]	+[l]
Bladder	+[r]	+[e]	+[l]
Cerebrum	−	−	+[o]

Superscripts indicate reactivities as follows: a, cortical epithelial cells; b, cortical and medullary epithelial cells; c, subpopulation of cortical and medullary epithelial cells; blood vessels; d, high endothelial venules; e, all epithelial cell layers in stratified epithelium; f, dermis and subcutis; g, goblet cells and crypt cells; h, all epithelial cells in crypts and villi; i, lamina propria; j, parenchymal cells; k, secretary ducts and basal parts of alveolar cells; l, interstitial connective tissue; m, thin loops of Henle; n, capillaries, glomeruli; o, capillaries, p, type 2 pneumocytes; q, respiratory and terminal bronchioles, and r, umbrella cells. ND, not done.

endothelial venules (HEV), the site of entry for lymphoid cells in the lymph node (data not shown).

Immunohistology of scFvs with Nonlymphoid Tissues. To further analyze the specificity of the three cloned scFvs, a comparative immunohistological analysis using serial sections of various organs was performed. Reactivity patterns are shown in Fig. 3 and summarized in Table 1.

Fig. 3 shows the reactivity of scFvs from TB4–4 (*a* and *b*), TB4–20 (*c* and *d*), and TB4–28 (*e* and *f*) with duodenum (*a*, *c*, and *e*) and bladder (*b*, *d*, and *f*).

In the duodenum, TB4–4 scFvs strongly react with isolated cells in crypts and villi (Fig. 3*a*). Close inspection revealed specific reactivity with goblet cells. In addition, a subset of columnar epithelial cells in the crypts is stained by scFvs of this MoPhab. TB4–4 scFvs also crossreact to a subset of epithelial cells in the superficial layer of the urothelium in the bladder, leaving the basal epithelial cells negative (Fig. 3*b*).

In contrast to TB4–4, TB4–20 scFvs react with all epithelial cells in the duodenum, both in crypts and in villi (Fig. 3*c*). These scFvs detect all epithelial layers in the urothelium of the bladder (Fig. 3*d*).

ScFvs from MoPhab TB4–4 and TB4–20 scFvs also differ in their reactivity with keratinized stratified epithelium in the murine and human skin. Whereas TB4–4 scFvs are completely unreactive, TB4–20 scFvs show a strong reaction with all cell layers in the epidermis (data not shown).

ScFvs obtained from MoPhab TB4–28 react with the apical side of the epithelial cells in the duodenum. They also detect the lamina propria in the duodenum (Fig. 3*e*) and in the bladder (Fig. 3*f*).

Confocal Microscopy with scFvs. To determine whether determinants detected by the three types of scFvs were expressed at the cell surface or in the cytoplasm of thymic epithelial cells, we studied 25-μm-thick frozen sections incubated with scFvs, using CLSM (Fig. 4). This study revealed that TB4–4 and TB4–20 scFvs detect epitopes expressed in the cytoplasm of epithelial cells. A fine lacework of cytoplasmic filaments can be observed in all cortical epithelial reticular cells (Fig. 4 *a* and *b*) and, for TB4–20, also in all medullary epithelial cells (data not shown).

ScFvs of MoPhab TB4–28 detect isolated groups of epithelial reticular cells in both the cortex and the medulla. Such epithelial cells show thin diffusely stained cytoplasmic extensions. They are frequently found in close proximity to or in contact with capillaries, which themselves also strongly react with TB4–28 (Fig. 4*c*). By studying a series of planes through the 25-μm-thick section we observed a continuous diffuse staining pattern, encompassing the total width of the of cytoplasmic process, indicating that the molecules detected by this scFv are expressed at, or in close proximity to, the cell surface.

Immunocytology of scFvs with Cultured Thymic Epithelial Cells. To confirm the subcellular localization of the epitopes detected by our scFvs, we examined their reactivity in cultured thymic epithelial cells, using fluorescence microscopy (Fig. 5). This study in part confirmed the CLSM data, in that TB4–4 scFvs react with approximately 75% of the cultured cells (Fig. 5*a*), whereas TB4–20 scFvs react with all thymic epithelial cells in culture (Fig. 5*b*), while both scFvs label cytoplasmic filaments. In contrast, scFvs from MoPhab TB4–28 did not react, beyond the detection level, with cultured thymic epithelium (Fig. 5*c*). Apparently, the molecule recognized by TB4–28 is lost during the 7-day culture period.

Reactivity of scFvs and $(scFv)_2$ in Western Blots. For an initial characterization of the molecules detected by the three scFvs we performed Western blotting of solubilized stromal cells, obtained either from 7-day cultured fetal thymi or from adult freshly prepared thymic stroma derived from BALB/c thymi. For all three scFvs we were able to detect specific bands. TB4–4 detects a broad band with a molecular mass of around 46 kDa; TB 4–20 detects a band of 50 kDa, and TB4–28 detects a doublet in the range of 30 kDa (data not shown).

Footprint Analyses and DNA Sequencing. *Bst*N1 footprint analysis of the three MoPhabs showed a similar pattern for MoPhabs TB4–4 and TB4–20 and a different pattern for TB4–28 (data not shown). The sequencing data presented in Table 2 show that the three MoPhabs have entirely different CDR3 regions in their heavy chains, varying in length between 6 and 12 amino acids. All three MoPhabs express a Vλ3 light chain.

DISCUSSION

The present study shows that the phage display technology can be applied to isolate scFvs directed to cell types forming an integral part of lymphoid organs. Thus, by subtractive isolation, using, on one hand, thymocytes and splenocytes as adsorber cells and, on the other hand, intact, mildly fixed thymic stroma as target tissue, we were able to isolate MoPhabs reactive with thymic stromal cell types, while MoPhabs to lymphoid cells were not detected.

For several reasons mild fixation of the thymic stroma seems advantageous in this selection procedure. First, the antigenicity of determinants expressed by stromal cells is preserved (20). Second, fixation prevents internalization of antigens recognized by MoPhabs during overnight incubation of the tissue with the phage library. Finally, fixation inhibits loss of antigenicity by proteolytic enzymes present in the intact tissue fragments. The present short fixation period is essential in the procedure, because it still provides the possibility of removing unbound thymocytes from the fragments by vigorous rinsing of the tissues, thus exposing the thymic stromal cells for phage selection.

Although our selection method was aimed to isolate MoPhabs directed to cell surface determinants expressed on intact thymic stromal cells, several of the isolated MoPhabs recognized molecules expressed in the cytoplasm of stromal cells. This result may be inherent to the present procedure: after fixation, the thymus was cut into fragments, thus exposing cytoplasmic determinants.

To avoid isolation of MoPhabs directed to MHC antigens, we decided to change the MHC haplotype of the mouse strain in each selection round. This measure appeared successful, because so far we have been unable to detect MHC-specific MoPhabs. Furthermore, the present procedure led to the isolation of MoPhabs crossreacting to thymic stromal cells in human tissues, showing that evolutionarily conserved mole-

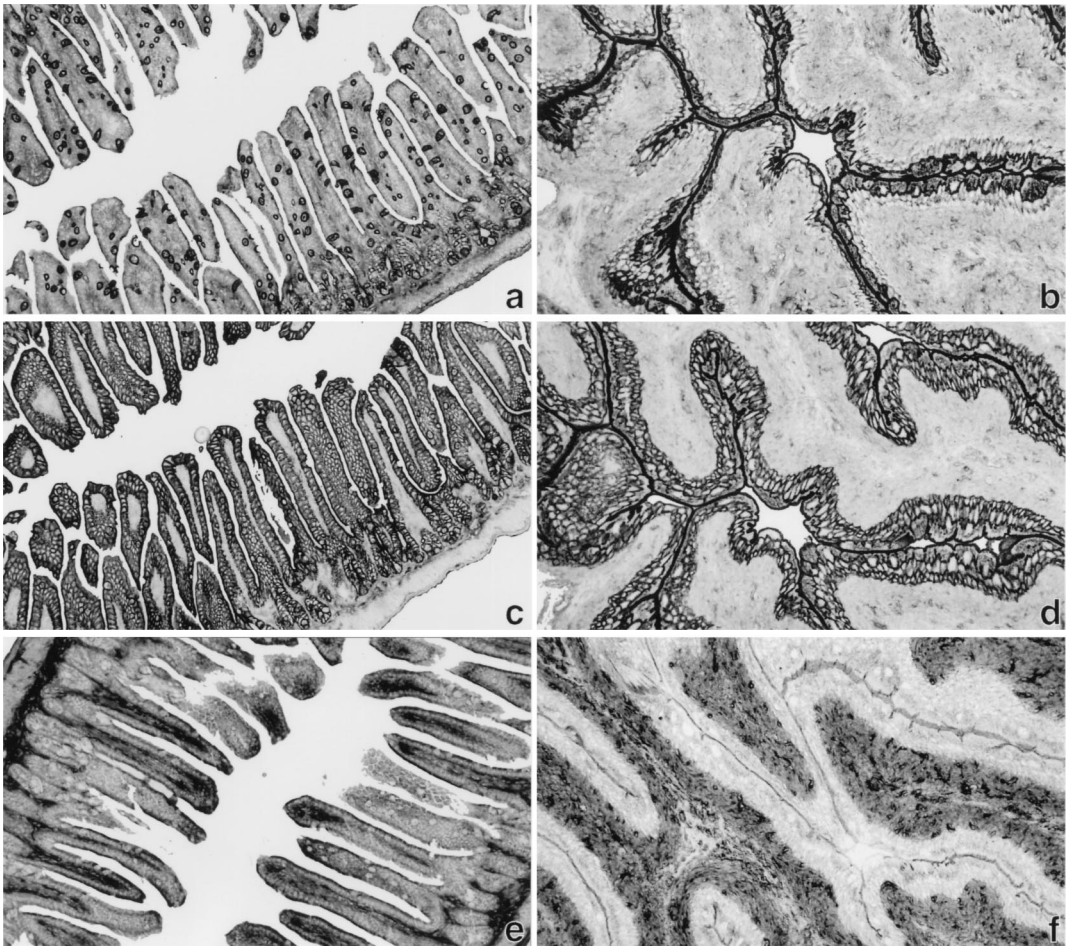

FIG. 3. Frozen sections of mouse duodenum (*a*, *c*, and *e*) and bladder (*b*, *d*, and *f*) incubated with scFvs derived from MoPhabs TB4–4 (*a* and *b*), TB4–20 (*c* and *d*), and TB4–28 (*e* and *f*). (×84.)

cules, to which the immune system is generally tolerant, can be picked up by the phage display method.

On the basis of their staining patterns, two of our scFvs can be grouped with monoclonal antibodies recognizing subsets of epithelial cells according to so-called CTES patterns (8). scFvs from MoPhab TB4–20 react with both cortical and epithelial thymic reticular cells, like a CTES I pattern. scFvs from MoPhab TB4–4 react with cortical epithelial cells and a minor subset of medullary epithelial cells, resembling a CTES III pattern.

scFvs of MoPhab TB4–28 do not fit in the present CTES patterns. Both our confocal microscopic studies and immunofluorescence labeling of overnight cultured thymic stromal cells (W.V.E., G. Anderson, and E. J. Jenkinson, unpublished work) indicate that the antigen detected by TB4–28 is expressed at the cell surface of a small subpopulation of epithelial cells. Apparently, the molecule detected by TB4–28 is not consistently expressed by thymic epithelial cells, since cell culture for the period of 7 days leads to loss of expression of the TB4–28 antigen.

TB4–4 and TB4–20 scFvs are not thymus-specific; they also recognize epitopes expressed in other epithelia. In gut epithelium, TB4–20 reacts with all cell types in both crypts and villi, while TB4–4 recognizes goblet cells and a subpopulation of epithelial cells located at the bottom of the intestinal crypts. The latter cells are probably epithelial stem cells or immature differentiating epithelial cells (21). This observation indicates that our scFvs discriminate between the two major differentiation lineages of epithelial cells: absorptive cells are detected by TB4–20 scFvs, and goblet cells are detected by TB4–4 scFvs. Strikingly, such "classical" epithelial cells also occur in the thymus of immunodeficient mice, where T cell development is arrested at a very early stage, such as CD3 transgenic mice (5) and Ikaros −/− mice. Such mice show thymic cysts, in which goblet cells react with TB4–4, while the remaining epithelial cells are all positive for TB4–20 (W.V.E., unpublished results).

The reactivity patterns of our scFvs add information to studies on the morphogenesis of the thymus. In rodents,

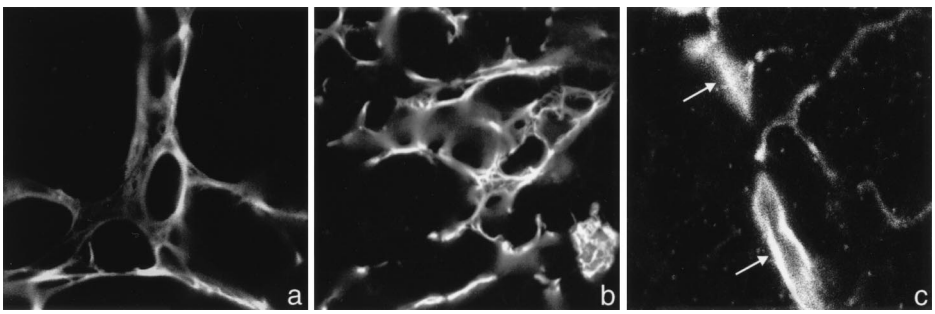

FIG. 4. CLSM of a frozen section of the mouse thymus, incubated with scFvs derived from MoPhabs TB4–4 (*a*), TB4–20 (*b*), and TB4–28 (*c*). Note staining of cytoplasmic filaments in *a* and *b*. The arrows in *c* indicate a capillary. (×700.)

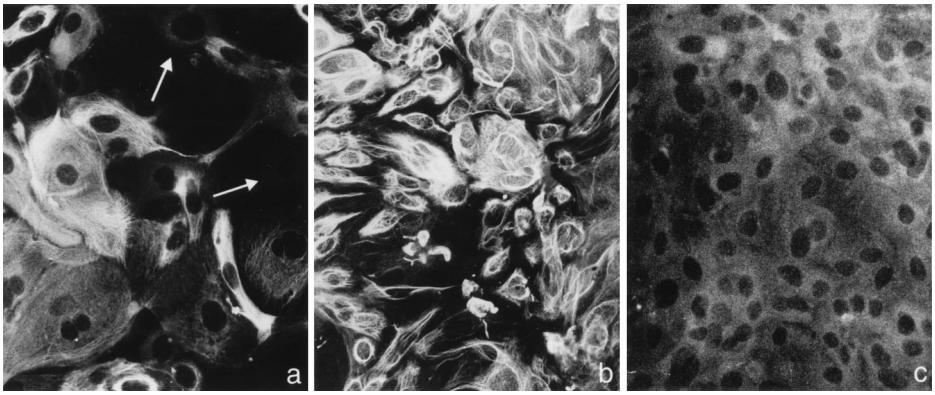

FIG. 5. Fluorescence microscopy of *in vitro* cultured thymic epithelial cells, incubated with scFvs derived from MoPhabs TB4–4 (*a*) TB4–20 (*b*), and TB4–28 (*c*). The arrows in *a* indicate epithelial cells negative for TB4–4. (×310.)

published data indicate that thymic tissue arises from contributions of the ectoderm and endoderm from the third pharyngeal cleft and pouch respectively (22, 23). The two tissues are separated from each other by a thin layer of mesenchyme, originating from the cephalic neural crest (24). Epithelial–mesenchymal interaction then leads to the development of a thymic primordium (25), where cortical and medullary epithelial cells are already positioned at day 14 of gestation (26). The relation between the two classes of epithelial cells and the three germ layers is still obscure. Cordier and Haumont (22) have argued that cortical epithelial cells are ectodermal in origin, whereas medullary epithelial cells derive from the endoderm. Others describe a mixed (endo–ectodermal) origin for cortical epithelial cells (27). Our results obtained with TB4–4 scFvs, staining both the thymic cortex and other endoderm-derived epithelia, indicates an endodermal contribution to the development of the thymic cortex. This idea is further supported by a recent study from Wallin *et al.* (28) describing the expression of the transciptional regulatory protein Pax-1. During embryogenesis, Pax-1 is expressed in the early endoderm, including the epithelium of the third pharyngeal pouch. In the adult thymus, Pax-1 is expressed in a subpopulation of cortical epithelial cells, again indicating that the development of the cortex is influenced by endoderm-derived cells. Pax-1 is also controlling the tertiary structure of the thymic stroma, because mutations in the *Pax-1* gene create the appearance of thymic cysts, concomitant with a decreased capacity of the thymus to support T cell development.

Besides Pax-1 the winged helix *nude* gene product plays a crucial role in the architecture of the thymic stroma, because a targeted disruption of this gene leads to a complete loss of the epithelial network, leaving the thymus as two cysts lined by "classical" epithelial cells (29). Both types of experiments clearly indicate that the tertiary structure of thymic stromal microenvironments is controlled by genes expressed within epithelial cells. However, from experiments with various types of immunodeficient mice, it has recently become clear that lymphoid cells also contribute to the organization of the thymic stroma. At the level of both the cortex and the medulla, developing lymphocytes influence stromal differentiation and the organization of the three-dimensional composition of the thymic stroma, a phenomenon designated "thymic crosstalk" (7). In this context, the plasticity of the thymic stroma is further illustrated by the recent discovery of thymic stromal "stem" cells—i.e., epithelial cells with the potential capacity to differentiate into either cortical or medullary epithelial cells (14).

We are currently investigating whether the subtractive approach, using intact thymus fragments, can be applied to unveil putative differences of thymic stromal microenvironments present in transgenic and knock-out mice where T cell differentiation is arrested at discrete early stages.

Table 2. Deduced amino acid sequence of complementarity-determining region 3 (CDR_3) and the usage of V_H and V_L genes by the selected scFvs

MoPhab	CDR_3	V_H	V_L
TB4-4	ALYMMP	DP 45	Vλ3
TB4-20	DYQSYHGSWFDS	DP 47	Vλ3
TB4-28	SPLPIYFDY	DP 14	Vλ3

Assignment of germ-line V_H and V_L segments is according to the V-BASE sequence directory described by Tomlinson *et al.* (19), Medical Research Council Centre for Protein Engineering, Cambridge, U.K.

We thank Dr. R. Willemse and Mrs. L. Wiegman for technical assistance. Mr. T. van Os and Dr. A. Houtsmuller are acknowledged for computer graphics and CLSM assistance. Finally, typographical assistance was kindly provided by Mrs. E. van Eenennaam. This experimental work was in part supported by the Netherlands Organization for Scientific Research (NWO), Grant 900-505-273.

1. Van Ewijk, W. (1991) *Annu. Rev. Immunol.* **9,** 591–615.
2. Owen, J. J. T. & Moore, N. C. (1995) *Immunol. Today* **16,** 336–338.
3. Anderson, G., Owen, J. J. T., Moore, N. C. & Jenkinson, E. J. (1994) *J. Exp. Med.* **179,** 2027–2031.
4. Martin-Fontecha, A., Schuurman, H. J. & Zapata, A. (1994) *Thymus* **22,** 201–213.
5. Holländer, G. A., Wang, B., Nichogiannopoulou, A., Platenburg, P. P., Van Ewijk, W., Burakoff, S. J., Gutierrez Ramos, J. C. & Terhorst, C. (1995) *Nature (London)* **373,** 350–353.
6. Shores E. W., Van Ewijk, W. & Singer, A. (1991) *Eur. J. Immunol.* **21,** 1657–1661.
7. Van Ewijk, W., Shores, E. W. & Singer, A. (1994) *Immunol. Today* **15,** 214–217.
8. Brekelmans, P. & Van Ewijk, W. (1990) *Semin. Immunol.* **2,** 13–24.
9. Kruisbeek, A. M., Mond, J. J., Fowlkes, B. J., Carmen, J. A., Bridges, S. & Longo, D. L. (1985) *J. Exp. Med.* **161,** 1029–1047.
10. Kyewski, B. A., Schirrmacher, V. & Allison, J. P. (1989) *Eur. J. Immun.* **19,** 857–863.
11. McDuffie, M., Born, W., Marrack, P. & Kappler, J. (1986) *Proc. Natl. Acad. Sci. USA* **83,** 8728–8733.
12. de Kruif, J., Terstappen, L., Boel, E. & Logtenberg, T. (1995) *Proc. Natl. Acad. Sci. USA* **92,** 3938–3942.
13. de Kruif, J., Boel, E. & Logtenberg, T. (1995) *J. Mol. Biol.* **248,** 97–105.
14. Röpke, C., van Soest, P., Platenburg, P. P. & Van Ewijk, W. (1995) *Dev. Immunol.* **4,** 149–156.
15. Van Vliet, E., Melis, M. & Van Ewijk, W. (1984) *Eur. J. Immunol.* **14,** 524–529.
16. Van Ewijk, W. (1988) *Lab. Invest.* **59,** 579–590.
17. Gu, J., Stephenson, C. G. & Iadarola, M. J. (1994) *Biotechniques* **17,** 257–260.
18. Berendes, P., Hoogeveen, A., Van Dijk, M., Van Denderen, J. & Van Ewijk, W. (1995) *Leukemia* **9,** 1321–1327.
19. Tomlinson, I. M., Walter, G., Marks, J. D., Llewelyn, M. B. & Winter, G. (1992) *J. Mol. Biol.* **227,** 776–798.
20. Van Ewijk, W., Coffman, R. C. & Weissman, I. L. (1980) *Histochem. J.* **12,** 349–361.
21. Paulus, U., Loeffler, M., Zeidler, J., Owen, G., Potten, C. S. (1993) *J. Cell. Sci.* **106,** 473–483.
22. Cordier, A. C. & Haumont, S. M. (1980) *Am. J. Anat.* **157,** 227–263.
23. Owen, J. J. T. & Jenkinson, E. J. (1984) *Am. J. Anat.* **170,** 301–310.
24. Bockman, D. E. & Kirby, M. L. (1984) *Science* **223,** 498–500.
25. Auerbach, R. (1960) *Dev. Biol.* **2,** 271–284.
26. Van Vliet, E., Jenkinson, E. J., Kingston, R., Owen, J. J. T. & Van Ewijk, W. (1985) *Eur. J. Immunol.* **15,** 675–681.
27. Crisan, C. (1935) *Z. Anat. Entwicklungsgesch.* **104,** 327–358.
28. Wallin. J., Eibel, H., Neubüser, A., Wilting, J., Koseki, H. & Balling, R. (1996) *Development* **122,** 23–30.
29. Nehls, M., Kyewski, B., Messerle, M., Waldschütz, B., Schüddekopf, K., Smith, A. J. H. & Boehm, T. (1996) *Science* **272,** 886–889.